Misfit dislocations in nanoscale ferroelectric heterostructures

V. Nagarajan, C. L. Jia, H. Kohlstedt, and R. Waser
Institut für Festkörperforschung (IFF), Forschungzentrum Jülich D 52425, Germany

I. B. Misirlioglu and S. P. Alpay[a)]
Department of Materials Science and Engineering, Institute of Materials Science,
University of Connecticut, Storrs, Connecticut 06269

R. Ramesh
Department of Materials Science and Engineering and Department of Physics, University of California,
Berkeley, California 94720

We present a quantitative study of the thickness dependence of the polarization and piezoelectric properties in epitaxial (001) $PbZr_{0.52}Ti_{0.48}O_3$ films grown on (001) $SrRuO_3$-buffered (001) $SrTiO_3$ substrates. High-resolution transmission electron microscopy reveals that even the thinnest films ($\sim$8 nm) are fully relaxed with a dislocation density close to 10^{12} cm^{-2} and a spacing of approximately 12 nm. Quantitative piezoelectric and ferroelectric measurements show a drastic degradation in the out-of-plane piezoelectric constant (d_{33}) and the switched polarization (ΔP) as a function of decreasing thickness. In contrast, lattice-matched ultrathin $PbZr_{0.2}Ti_{0.8}O_3$ films that have a very low dislocation density show superior ferroelectric properties. Supporting theoretical calculations show that the variations in the strain field around the core of the dislocation leads to highly localized polarization gradients and hence strong depolarizing fields, which result in suppression of ferroelectricity in the vicinity of a dislocation. © *2005 American Institute of Physics.* [DOI: 10.1063/1.1922579]

Understanding nanoscale ferroelectrics has become a topic of intense fundamental research.[1,2] Recent studies show that lattice engineering and internal stresses have a major role in the structural and physical properties of ultrathin ferroelectric films.[3–5] In lattice-matched (or epitaxial) films and heterostructures, the strain due to lattice mismatch between the film and the substrate can be relaxed during film growth. by the formation of orthogonal arrays of misfit dislocations at the film-substrate interface.[6–11] For epitaxial 10 nm high $PbZr_{0.52}Ti_{0.48}O_3$ [PZT (52/48)] nanoislands on Nb-doped $SrTiO_3$ (STO), the strain field associated with the dislocation core was found to be propagating into the ferroelectric layer with a height of $\sim$4 nm and a width of $\sim$8 nm, a significant volume fraction of the islands.[4]

Recent theoretical results[12] for an epitaxial PTO thin film with periodic misfit dislocations predict that the strong coupling of the dislocation strain field with the polarization leads to high local polarization gradients. This results in strong depolarizing fields around a dislocation in a region of 5–10 nm in diameter around the core, that ultimately suppress ferroelectricity.[13,14] Misfit dislocations should thus act as an extrinsic dominating factor in the scaling of polarization and all physical properties as a function of thickness. In this letter, we provide a systematic quantitative study on the role of dislocations on the stability ferroelectricity in epitaxial ferroelectric thin films.

Epitaxial (001) PZT (52/48) films were grown on (001) $SrRuO_3$ (SRO)-buffered (001) $SrTiO_3$ (STO) substrates. The thickness of the PZT (52/48) layer was varied from 200 nm down to 12 nm thickness. The details of the growth method and parameters are given elsewhere.[15] In order to compare

and contrast the effect of misfit dislocations, very well lattice-matched PZT (20/80)/SRO/STO heterostructures were also prepared from 80 nm down to 4 nm. In order to avoid complications from 90° domain formation,[16] we chose 80 nm as the upper bound for the PZT (20/80) films.

X-ray synchrotron measurements confirmed that the SRO layer was pseudomorphic with the STO substrate with an in-plane lattice parameter of 0.3905 nm at room temperature (RT) and 0.3930 nm at the growth temperature T_G =600 °C. Additional x-ray and high-resolution transmission electron microscopy (TEM) diffraction verified the epitaxial orientational relationship: (001)PZT[100]PZT∥(001)SRO [100]STO∥(001)STO[100]STO. X-ray diffraction reciprocal space mapping (not shown) of the PZT layers confirmed them to be tetragonal. At T_G, the lattice parameter of PZT (52/48) is 0.4084 nm; therefore, the misfit between SRO and PZT (52/48) at T_G is -3.93%. Employing the Matthews–Blakeslee criteria[6] and using the elastic moduli of PZT (52/48),[17] the critical thickness for misfit dislocation formation was calculated to be $\sim$2.3 nm and the nominal dislocation spacing to be 12.8 nm for the 12 nm and 10.5 nm for the 160 nm thick film, respectively. In contrast, the in-plane lattice parameter for PZT (20/80) at T_G is 0.396 nm; thus, the lattice mismatch at growth temperature is only around -0.7% resulting in a theoretical $h_c \sim 10$ nm and a spacing of about 30 nm.

Figure 1(a) is a representative cross-sectional, TEM image of a 20 nm thick PZT (52/48) film on SRO/STO. The ferroelectric layer is rough even at the nanoscale and has a large density of dislocations indicated by the strain contrast in the image. In comparison, Fig. 1(b) is a low-magnification image of a 20 nm thick PZT (20/80) film. The dashed lines in Fig. 1(b) indicate the interfaces between the PZT, SRO, and STO layers, respectively. The interfaces are smoother

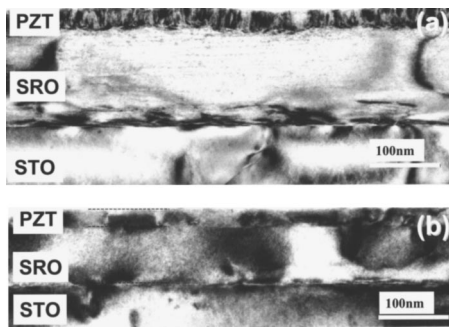[a)]Author to whom correspondence should be addressed; electronic mail: p.alpay@ims.uconn.edu

FIG. 1. Comparison of TEM images for PZT (52/48) (top) and PZT (20/80) (bottom) films, both 20 nm thick. The image shows that PZT (52/48) has a large density of dislocations and rough interfaces due to lattice mismatch. PZT (20/80) film shows a relatively smooth and sharp interface as a result of the closer lattice matching.

with a significantly reduced strain contrast and the density of defects is greatly reduced. Figure 2(a) shows a high-resolution image of an 8 nm thick PZT (52/48) sandwiched between the top and bottom SRO layers. An array of misfit dislocations is observed at the interface between the PZT (52/48) and the bottom SRO layer as indicated by open arrows. The majority of the dislocations are located in the SRO layer away from the interface plane. Some of the dislocations dissociate into two partials to lower the energy associated with the lattice strain. Figure 2(b) shows a magnified region around the dislocation core within the white frame. Dissociation of the dislocation can be clearly seen as indicated by two arrows. The corresponding Burger's vectors for the two dissociating edge-type partials are $a/2$ [101] and $a/2$ [10$\bar{1}$], leading to a sum Burger's vector $\mathbf{b} = a$[100].

Lattice strain in the vicinity of the dislocation was studied by studying the changes in lattice fringe spacings using geometric phase analysis of the lattice fringe image.[18] In calculating the lattice spacing variations in the framed area
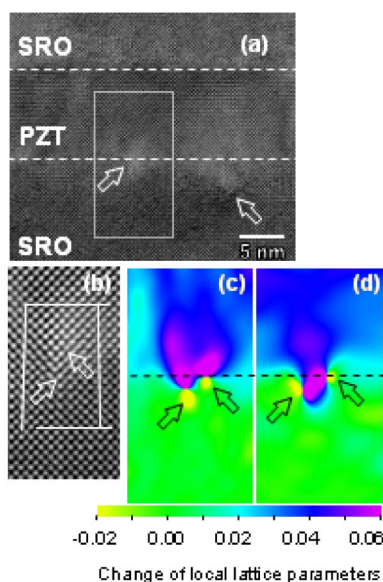

FIG. 2. (Color online) (a) HRTEM image of a 8 nm SRO/PZT(52/48)/SRO heterostructure. The arrows point toward misfit dislocations. The dislocation has split into two partials to further reduce the energy associated with the lattice strain. (b) A magnified region around the dislocation core within the white frame. Dissociation of the dislocation into two partials can be clearly seen as indicated by two arrows. (c) and (d) show maps of spacing changes along the in-plane axis [100] and out-of-plane axis [001], respectively.
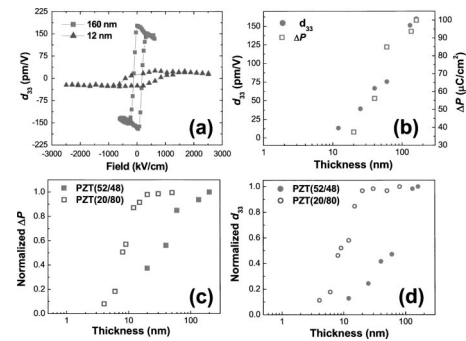

FIG. 3. Piezoelectric and polarization characterization of the PZT (52/48) and PZT (20/80) thickness series: (a) Piezoelectric hysteresis loops for the 12 nm (triangles) and 160 nm (squares) PZT (52/48) films. (b) Measured out-of-plane piezoelectric constant d_{33} and switchable polarization (ΔP) for PZT (52/48) as a function of film thickness. (c) Out-of-plane d_{33} and (d) switchable polarization normalized with respect to their individual "unsuppressed" values as a function of film thickness. In the case of the PZT (52/48) films, a steep drop begins at $\sim$100 nm, a thickness much greater than the case of the PZT (20/80) film ($\sim$12 nm).

of Fig. 2(b), the SRO lattice fringes in the bottom part of the frame were used as a spacing reference. Figures 2(c) and 2(d) show the maps of spacing changes along the in-plane axis [100] and out-of-plane axis [001], respectively. The scale in Figs. 2(c) and 2(d) quantifies the changes in the local lattice parameter with respect to the SRO fringes. It can be seen that the SRO layer is locally compressed while the PZT layer has significant in-plane tensile strain close to the core. The extra half-plane is in the SRO layer with the core penetrating into this layer away from the interface to minimize excessive elastic energy associated with the core. This is frequently observed in films on substrates where the film is elastically stiffer than the substrate.[19] The abrupt changes of lattice stain, from compressive to tensile across the edge dislocation cores, are well characterized by variations in the color scale. Above the dislocation core, a tensile lattice strain is clearly seen in the two maps in comparison with the areas away from the dislocation cores and parallel to the interface. The lattice expansion in-plane is stronger than the one out-of-plane and extends far into the PZT (52/48) layer.

Quantitative piezoresponse force microscopy was used to extract the out-of-plane piezoelectric coefficient d_{33}. To ensure a uniform electric-field distribution, the measurements were made using a top electrode and a conductive Pt–Ir tip. The displacement of the cantilever was calibrated using x-cut quartz, which has a known piezoelectric coefficient (2.3 pm/V). Figure 3(a) shows d_{33} loops for two PZT (52/48) thicknesses: 12 nm (triangles) and 160 nm (squares) thick films. The plot shows a dramatic reduction in the piezoelectric coefficient for the 12 nm film compared to the 160 nm thick film. For this composition, d_{33} for a clamped (001)-oriented epitaxial film without any suppression or extrinsic effects, is expected to be $\sim$157 pm/V (Ref. 20) as shown by the 160 nm thick film. This drops significantly for the 12 nm film, which shows average remanent d_{33} of only 30 pm/V. In Fig. 3(b), we plot d_{33} at remanence as a function of film thickness. It shows a systematic and sharp fall when the thickness is below 100 nm, indicating the detrimental effect of misfit dislocations. We also measured the switchable polarization (ΔP), which is the difference between the switched (P^*) and nonswitched ($P^{\hat{}}$) responses.[21] We used this instead of $2 \cdot P_R$, where P_R is the remanent polarization,
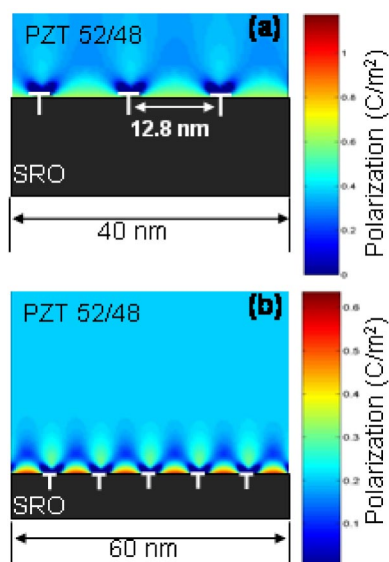
FIG. 4. (Color online) The polarization distribution around periodic misfit dislocations with $\mathbf{b}=a[\bar{1}00]$ in (a) 12 nm and (b) 200 nm thick (001) PZT (52/48) film on (001) SRO-buffered (001) STO substrate, assuming a deposition temperature of 600 °C. Film areas shown in (a) and (b) represent 12 nm×40 nm and 30 nm×60 nm cross section across the film thickness in the *xz*-plane, respectively. Individual elements in the simulations were ∼0.4 nm.

as it is less likely to be convoluted by leakage. We find that similar to d_{33}, the ΔP also drops drastically for thicknesses below 100 nm. This drop begins at a thickness much greater than that predicted for fully commensurate ferroelectric heterostructures by theory[22,23] or experiments.[24] It, therefore, clearly illustrates the dominant extrinsic role dislocations play in the size effects of nanoscale ferroelectrics. This is evident in Figs. 3(c) and 3(d), where we compare d_{33} and ΔP values of the PZT (20/80) versus PZT (52/48). For the sake of comparing both compositions on one scale, the values have been normalized to the unsuppressed theoretical values. The lattice-matched PZT (20/80) system shows no scaling in d_{33} or ΔP down to 15 nm.[24] In comparison, the drop in the PZT (52/48) system is much sooner; thereby exhibiting the overriding role of dislocations in the size effects of ferroelectrics.

To probe this further, we carried out a thermodynamic analysis to investigate the role of dislocations in ferroelectric materials using a methodology based on a modified mean-field Landau–Devonshire formalism incorporating the elastic energy of the dislocations, its electromechanical coupling to the polarization, and the internal field due to polarization gradients given by Maxwell's relations. The details of this method are given elsewhere.[12] We analyzed the polarization distribution around misfit dislocations with $\mathbf{b}=a[\bar{1}00]$ in (001) PZT (52/48) films with 12 and 200 nm thickness on thick (001) STO substrates with fully relaxed SRO buffer layers (SRO/STO). The internal stresses due to lattice mismatch were coupled with the stress field of dislocations in the linear elastic limit. As shown in Figs. 4(a) and 4(b), due to strong strain gradients, there is a drastic variation in the polarization near the film-substrate interface that should result in the formation of ∼10 and ∼15 nm thick ferroelectrically dead layers in 12 and 200 nm films, respectively. These plots also display the thickness dependence of the dead

layer-to-film thickness ratio. As films get thicker, the equilibrium dislocation density increases and hence the dislocation periodicity decreases resulting in better relaxation of epitaxial stresses. The thickness of the dead layer depends on the dislocation density, which theoretically levels off above ∼100 nm in PZT (52/48) films on SRO/STO.

These results have several implications in terms of properties of ultrathin ferroelectric films and nanostructures. Obviously, there exists a significant volume that will not contribute to the polarization, dielectric, piezoelectric, and pyroelectric response. Furthermore, because of this dead layer, the applied electrical field that is necessary to activate the unique properties of ferroelectrics will be screened. These regions also serve as pinning centers for reversible 180° and non-180° domain-wall motion in the presence of an applied field, and thereby reduce the extrinsic contribution to all physical properties. The detrimental effect of such regions will be enhanced in nanoscale ferroelectric films and heterostructures, and hence play a critical extrinsic role in size effect studies of ferroelectrics.

[1]D. D. Fong, G. B. Stephenson, S. K. Streiffer, J. A. Eastman, O. Auciello, P. H. Fuoss, and C. Thompson, Science **304**, 1650 (2004).
[2]I. I. Naumov, L. Bellaiche, and H. Fu, Nature (London) **432**, 737 (2004).
[3]K. J. Choi, M. Biegalski, Y. L. Li, A. Sharan, J. Schubert, R. Uecker, P. Reiche, Y. B. Chen, X. Q. Pan, V. Gopalan, L. Q. Chen, D. G. Schlom, and C. B. Eom, Science **306**, 1005 (2004).
[4]M. W. Chu, I. Szafraniak, R. Scholz, C. Harnagea, D. Hesse, M. Alexe, and U. Gosele, Nat. Mater. **3**, 87 (2004).
[5]S. P. Alpay, I. B. Misirlioglu, A. Sharma, and Z.-G. Ban, J. Appl. Phys. **95**, 8118 (2004).
[6]J. W. Matthews and A. E. Blakeslee, J. Cryst. Growth **27**, 118 (1974).
[7]S. Stemmer, S. K. Streiffer, F. Ernst, and M. Ruhle, Phys. Status Solidi A **147**, 135 (1995).
[8]S. Y. Hu, Y. L. Li, and L. Q. Chen, J. Appl. Phys. **94**, 2542 (2003).
[9]L. Lymperakis, J. Neugebauer, M. Albrecht, T. Remmele, and H. P. Strunk, Phys. Rev. Lett. **93** 196401 (2004).
[10]G. F. Neumark, Phys. Rev. Lett. **21**, 1252 (1968).
[11]C. L. Canedy, H. Li, S. P. Alpay, L. Salamanca-Riba, A. L. Roytburd, and R. Ramesh, Appl. Phys. Lett. **77**, 1695 (2000).
[12]S. P. Alpay, I. B. Misirlioglu, V. Nagarajan, and R. Ramesh, Appl. Phys. Lett. **85**, 2044 (2004).
[13]A. M. Bratkovsky and A. P. Levanyuk, Phys. Rev. B **63**, 132103 (2001).
[14]A. M. Bratkovsky and A. P. Levanyuk, Phys. Rev. B **66**, 184109 (2002).
[15]C. L. Jia, J. R. Contreras, U. Poppe, H. Kohlstedt, R. Waser, and K. Urban, J. Appl. Phys. **92**, 101 (2002).
[16]S. P. Alpay and A. L. Roytburd, J. Appl. Phys. **83**, 4714 (1998).
[17]*Landolt-Börnstein, Numerical Data and Functional Relationships in Science and Technology* (Springer, Berlin, 1982).
[18]M. J. Hytch, E. Snoeck, and R. Kilaas, Ultramicroscopy **74**, 131 (1998).
[19]X. Wu and G. C. Weatherly, Semicond. Sci. Technol. **18**, 307 (2003).
[20]L. Chen, V. Nagarajan, R. Ramesh, and A. L. Roytburd, J. Appl. Phys. **94**, 5147 (2003).
[21]P. K. Larsen, G. L. M. Kampschoer, M. J. E. Ulenaers, G. A. C. M. Spierings, and R. Cuppens, Appl. Phys. Lett. **59**, 611 (1991).
[22]J. Junquera and P. Ghosez, Nature (London) **422**, 506 (2003).
[23]A. G. Zembilgotov, N. A. Pertsev, H. Kohlstedt, and R. Waser, J. Appl. Phys. **91**, 2247 (2002).
[24]V. Nagarajan, S. Prasertchoung, T. Zhao, H. Zheng, J. Ouyang, R. Ramesh, W. Tian, X. Q. Pan, D. M. Kim, C. B. Eom, H. Kohlstedt, and R. Waser, Appl. Phys. Lett. **84**, 5225 (2004).